PROCEEDINGS OF SPIE

SPIEDigitalLibrary.org/conference-proceedings-of-spie

Core-shell (TiO2@Silica) nanoparticles for random lasers

E. Jimenez Villar, Valdeci Mestre, N. U. Wetter, Gilberto F. de Sá

E. Jimenez Villar, Valdeci Mestre, N. U. Wetter, Gilberto F. de Sá, "Core-shell (TiO2@Silica) nanoparticles for random lasers," Proc. SPIE 10549, Complex Light and Optical Forces XII, 105490D (22 February 2018); doi: 10.1117/12.2289228

SPIE.

Event: SPIE OPTO, 2018, San Francisco, California, United States

Core-shell (TiO_2@Silica) nanoparticles for random lasers

E. Jimenez-Villar*[a,b], Valdeci Mestre[c], N. U. Wetter[a], Gilberto F. de Sá[d]
[a]Instituto de Pesquisas Energéticas e Nucleares, CNEN_IPEN, Rua Prof. Lineu Prestes 2242− Cidade Universitaŕia, São Paulo, SP, Brazil 05508-000; [b]Departamento de Física aplicada, IFGW, Universidade Estadual de Campinas, Campinas, SP, Brazil 13083-859, [c]CCEA, Universidade Estadual da Paraíba, Patos, PB, Brazil 58706-560, [d]Departamento de Química Fundamental, Universidade Federal de Pernambuco, Recife, PE, Brazil 50670-901
**Ernesto.Jimenez@uv.es*

ABSTACT

Scattering media are of great current interest, due to their potential applications in photovoltaic cells, efficient photocatalyzers, random lasers and novel optical functional devices. Here, we have introduced a core–shell scattering medium for random lasing composed by core-shell nanoparticles (TiO_2@Silica) suspended in an ethanol solution of Rhodamine 6G. Higher efficiency, lower laser threshold and long photobleaching lifetime were demonstrated in random laser. A promising method called fraction of absorbed pumping (*FAP*) has been introduced, which opens a new avenue to characterize and study scattering media. In this article, we also investigate the random laser action at the critical regime of localization by increasing considerably the concentration of TiO_2@Silica nanoparticles. Narrow peaks arising in the random laser emission spectrum are observed. The classical superfluorescence band of the random laser was measured separately by collecting the emission at the back of the samples, showing a linear dependence with pumping fluence without gain depletion. However, frontal collection showed the saturation of emission and absorption. The emission spectrum of the peak mode (localized modes) shows approximately equal intensity, indicating suppression of the interaction between the peaks modes. The linewidth of these peaks is lower than that of the passive modes of the scattering medium, which was attributed to an anomalous nonlinear increase of the refractive index by localization.

Keywords: Random laser, Anderson localization of light, photonic in disordered media, core-shell (TiO_2@Silica) nanoparticle, fluorescence of organic molecules.

1. INTRODUCTION

Strong disordered optical media are of great current interest, due to their potential applications in photovoltaic cells [1], random lasers [2–4], localization of light [5–8], and novel optical functional devices [9]. Here, we studied the random laser action in a colloidal suspension composed of core-shell TiO_2@Silica nanoparticles (NPs) suspended in an ethanol solution of Rhodamine 6G (R6G). By using a Stöber method [10], TiO_2 NPs were coated with a silica shell of ~40 nm thickness. The silica coating acts as a barrier to prevent charge transfer, avoiding the dye photodegradation effect [11,12]. Moreover, the silica shell prevents the "optical" junction of the TiO_2 scattering surfaces (steric "optical" effect), preserving the scattering strength of the medium [11]. We called this property optical colloidal stability. Additionally, the silica shell presents low density and provides a light-coupling enhancement with TiO_2 scattering cores [12], inertness [13,14], and high dispersibility [15–20], which has enabled their use in numerous applications [21–25]. For lower nanoparticle concentration [$5.6x10^{10}$ NPs ml^{-1}] (diffusive regime), we showed a random laser with high efficiency, a long photobleaching lifetime, narrower bandwidth and lower laser threshold than the traditional laser that uses only TiO_2. The random or powder laser was predicted by Letokhov in 1968 [26]. In the works reported by Noginov [27], Cao [28] and Wiersma [29], detailed reviews on random lasers can be found. Lawandy et al., who suspended TiO_2 nanoparticles in a conventional laser dye, obtained the first evidence of a random laser in solution [30]. The photodegradation effect and the inability to ensure complete colloidal dispersion, however, have limited the development and applications of such systems. TiO_2 NPs are prone to aggregate in aqueous solution, which limits extensively their application. Therefore, strong scattering particles coated with a silica shell of suitable thickness provides new opportunities for improving the operation of random lasers. For high nanoparticle concentration [$140x10^{10}$ NPs ml^{-1}] at the critical regime of approaching localization, narrow peaks arising in the RL emission spectrum are observed. This kind of peaks has been reported in systems composed by solid powders [31], porous gallium phosphide filled with liquid dye solution [32], sparse clusters [33], photonic crystals [34,35], and in low dimensional systems [36]. Spikes have also been observed over a broad range of

Complex Light and Optical Forces XII, edited by Enrique J. Galvez, David L. Andrews, Jesper Glückstad, Proc. of SPIE Vol. 10549, 105490D · © 2018 SPIE
CCC code: 0277-786X/18/$18 · doi: 10.1117/12.2289228

scattering strengths [37]. However, recent works [38,39] claim that, depending on the relative magnitude of the localization length and the system size, quasi modes and lasing modes may not be the same, and the statistical distribution of these emission spikes is an indication that under certain pumping conditions they do not correspond to true lasing with coherent feedback. Detailed reviews on this topic have been published elsewhere [40,41]. The study of the RL action at this critical regime of approaching localization is an open research frontier. It has been shown that a scattering medium with gain at the critical regime of approaching localization can lead to random lasing with coherent feedback [31,42], which besides being a fundamental topic [43] could also present significant applications [29].

2. MATERIALS AND METHODS

Samples preparation: For random laser studies at lower [NPs] [$5.6\text{x}10^{10}$ NPs ml^{-1}], two kinds of samples were prepared, both containing [$1\text{x}10^{-4}$M] of rhodamine 6G (R6G), one with TiO_2 and the other with TiO_2@Silica scattering nanoparticles. The silica coating onto TiO_2 NPs, with ~40 nm thickness and an irregular morphology, was made via a variant of the Stöber method [11]. For random laser studies at the critical regime of approaching localization, one sample with [$140\text{x}10^{10}$ NPs ml^{-1}] and containing [$1\text{x}10^{-4}$M] of R6G was used. In this case, the silica coating was made by an improved Stöber method and showed a regular morphology [44].
Random laser study: The pumping source of the random laser (RL) was the second harmonic of a Q-switched Nd:YAG (Continuum Minilite II, 25 mJ, 532 nm, with a pulse width of ~4 ns and a repetition rate up to 15 Hz), multimode, linearly polarized and with a spot size of 3 mm. For RL studies in the diffusive regime [$5.6\text{x}10^{10}$ NPs ml^{-1}], the emission spectra were collected through a multimode optical fiber (200 μm), coupled to a spectrometer (Ocean Optics, HR4000 UV-Vis) with a spectral resolution of 0.36 nm (FWHM). For RL studies at localization transition [$140\text{x}10^{10}$ NPs ml^{-1}], the emission spectra were collected through a multimode optical fiber (50-200 μm), coupled to a spectrometer (Ocean Optics, HR4000 UV-Vis) with a spectral resolution of 0.17 nm.

3. RESULTS AND DISCUSSION

3.1 Random laser study in the diffusive regime

Figure 1a and b show the behavior of the emitted intensity and the spectral width (FWHM), as a function of pumping energy fluence for the two kinds of scattering particle solutions (TiO_2 and TiO_2@Silica). As can be observed, the random laser action was improved for the system TiO_2@Silica, i.e. it presented a higher slope efficiency, narrower bandwidth and lower laser threshold. For the TiO_2@Silica system, the RL slope efficiency (RL_{eff}) was ~2.15 fold higher than for TiO_2. The laser threshold values extracted from the fittings (Fig. 1b, inflection point) for the TiO_2 and TiO_2@Silica systems were 2.28 ±0.04 mJ/cm^2 and 1.81 ±0.03 mJ/cm^2, respectively. The specular reflection measurements for both samples showed no difference; therefore, the coupling of pumping radiation with the samples is similar. A comparison between peak wavelengths of emission spectra, as a function of the pump fluence is found in Figure 1c for both systems (TiO_2 and TiO_2@Silica). The redshift of the RL spectrum with respect to the center of the luminescence spectrum at low pump intensity is almost null (<0.5 nm) for the TiO_2@Silica system at 120 mJ/cm^2. Therefore, it is inferred that the percentage of R6G molecules involved in the stimulated emission is close to 100%. The above results could be associated with a lower scattering mean free path (l_s), caused by a higher effective scattering surface (higher "optical" colloidal stability). This latter means that the pumping energy is confined in a smaller volume (higher effective pumping fluence). Moreover, the amount of R6G molecules inside this volume would also be lower and therefore a higher population inversion is achieved. l_s values measured for TiO_2 and TiO_2@Silica systems are 52 μm and 21 μm, respectively. The light of the pumping pulse reflected by the samples was measured with and without R6G. We designated the ratio between the pumping intensities reflected by the scattering medium with and without R6G as the fraction of absorbed pumping (*FAP*). *FAP* dependence with pumping energy fluence is shown in figure 1d (TiO_2 and TiO_2@Silica). For TiO_2@Silica system, *FAP* value for fluencies <0.3 mJ/cm^2, well below the laser threshold (FAP_{bT}), was constant (~4.7). The *FAP* value decreases for fluencies from ~0.3 down to ~1.8 mJ/cm^2. For fluencies >1.8 mJ/cm^2, *FAP* values remains approximately constant (~4.2). From the *FAP* value well below RL threshold (FAP_{bT}), we can estimate the average photon path length (l_{eO}) inside the scattering medium before being reflected from equation 1, where l_a is the ballistic or microscopic absorption length [R6G].

$$l_{eO} = l_a \ln(FAP_{bT}) \approx 384\ \mu\text{m} \times \ln(4.7) \approx 594\ \mu\text{m} \quad (1)$$

The l_a value well below the laser threshold (passive regime) should not change (384 μm at [10^{-4} M] of R6G). l_{eO} is much larger than l_s ≈21 μm, which would mean that the pumping photons undergo, on average, ~28 scattering events before being reflected. For the TiO_2 system, FAP_{bT} is approximately 2.5 and starts to decay at ~0.8 mJ/cm^2. Using equation 1,

one calculates l_{eO}≈352 μm. This means that pumping photons would undergo an average of only ~6.8 scattering events before being reflected, since l_s≈52 μm. This latter can explain the higher RL efficiency observed in the TiO_2@Silica system.

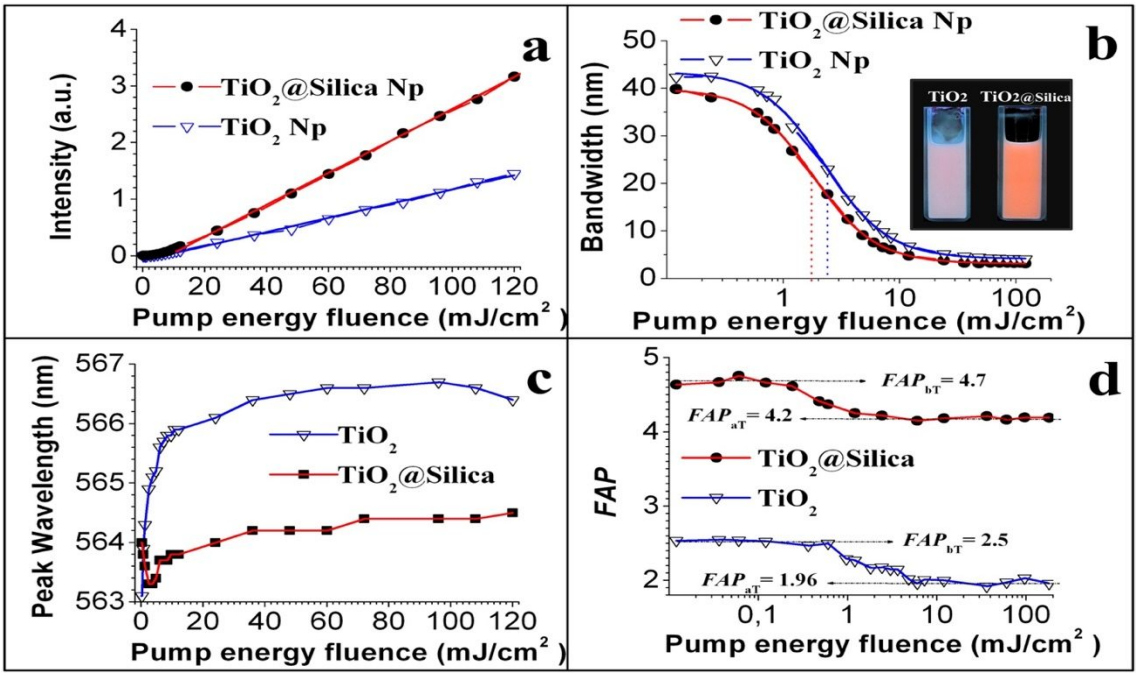

Figure 1. a) emitted peak intensity and (b) spectral FWHM emission of the RL for the two kinds of nanoparticles (TiO_2 and TiO_2@Silica). Inset of (b): photograph of ethanol solutions of R6G containing nanoparticles of TiO_2 and TiO_2@Silica. c-d) Influence of the pump energy fluence on c) peak wavelength of the emission spectrum and d) *FAP* values (*FAP* values for fluencies well below FAP_{bT} and above FAP_{aT} RL threshold are embodied in the graphic).

3.2 Random laser photodegradation

In order to study the RL photodegradation process, the laser beam of 3 mm diameter and fluence of 180 mJ/cm^2 was used to pump the samples, whose volume of 200 ml was accommodated in a 2 mm path length quartz cuvette. Figure 2a and b show a decrease in emission intensity with the number of shots. The TiO_2 system (fig. 2a) shows a rapid exponential decay. The number of shots for which the emission intensity decreased to 50% was 1540. However, for the TiO_2@Silica system (fig. 2b), the number of shots required was much higher (72000), which represents more than 46 times that of the TiO_2 system. The TiO_2 photocatalytic properties are a well-studied subject and have been used to remove or to degrade dyes from the environment [45].

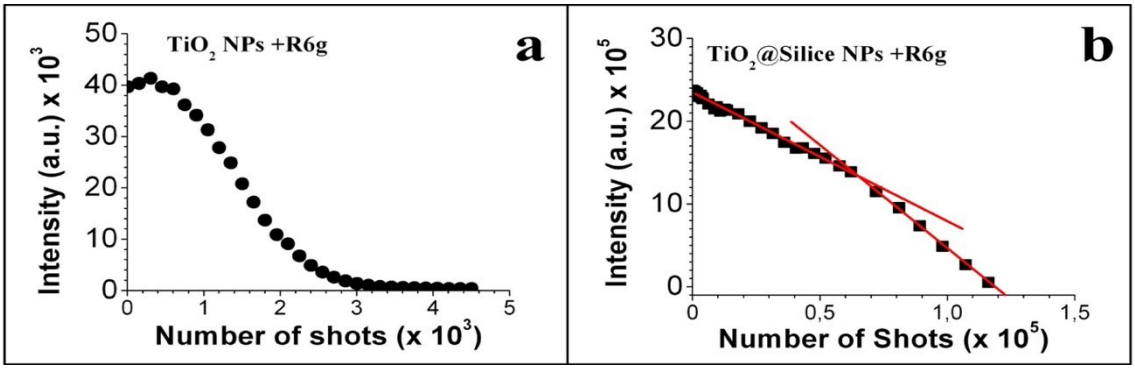

Figure 2. Photodegradation process of the RL action as a function of the number of shots (laser pumping fluence is 180 mJ/cm^2) for a) the TiO_2 system and b) the TiO_2@Silica system.

The photocatalytic pathway involves a reaction on the TiO_2 surface following several steps: 1) photogeneration of electron–hole pairs by exciting the semiconductor with >3.2 eV light; 2) separation of electrons and holes by traps existing on the TiO_2 surface; 3) a redox process induced by the separated electrons and holes with the adsorbates present on the surface. The exponential decreasing of the RL intensity in the TiO_2 system indicates that the photodegradation is proportional to its derivative, or as to the photodegradation rate. This means that the charge transfer and therefore the redox reaction will cause a greater charge transfer in the next laser shot. Thus, one might think that the high concentration of charges created by the TiO_2 nanoparticles at high pumping fluencies must react with the proper surface of the nanoparticles, reducing Ti^{4+} and oxidizing O^{2-}. This process results in oxygen vacancies [46], which act as traps for photo-electrons. These electrons trapped near the surface, act as a source of electron transfer coming from these superficial traps, increasing the efficiency of the redox process [47]. Additionally, the creation of oxygen vacancies in TiO_2 causes a progressive decreasing of the bandgap on the nanoparticles surface (TiO_2), which is reflected in the progressive increase in the creation of electron-hole pairs. This effect of photo-darkening is observed in films of TiO_2 exposed to the successive irradiation of the laser pulses [46]. The photodegradation process for TiO_2@Silica system presents a linear behavior. However, the modulus of the slope increases slightly after the emission intensity decreases to 50%. This fact indicates that the photodegradation rate of R6G remains constant until the emission intensity decreases to 50%. Subsequently, the photodegradation rate increases slightly, but remains constant. This phenomenon could be due to the decreased absorption of R6G, provoking an increase of the effective pumping fluence inside the scattering medium (TiO_2@Silica), which should increase the photodegradation rate of R6G.

3.3 Random laser action at the localization regime

3.3.1 Random laser action (frontal side)

In order to study RL action at localization, TiO_2@Silica NPs at [$140x10^{10}$ NPs ml^{-1}] were suspended in an ethanol solution with [$1x10^{-4}$ M] of R6g. Figure 3a shows the behavior of the emitted intensity as a function of pumping energy fluence. As can be observed, the RL slope efficiency (RL_{eff}) is not constant, it decreases markedly for pumping fluencies from ~12 up to 36 mJ/cm^2, showing a saturation of the emission. The green line represents the RL_{eff} for fluencies <12 mJ/cm^2. For pumping fluencies ≥36 mJ/cm^2, RL_{eff} adopts a 2.3 times smaller value (blue line). The RL threshold, determined by extrapolating the straight line corresponding to RL_{eff} (green line) to a zero emission intensity, is ~1.2 mJ/cm^2.

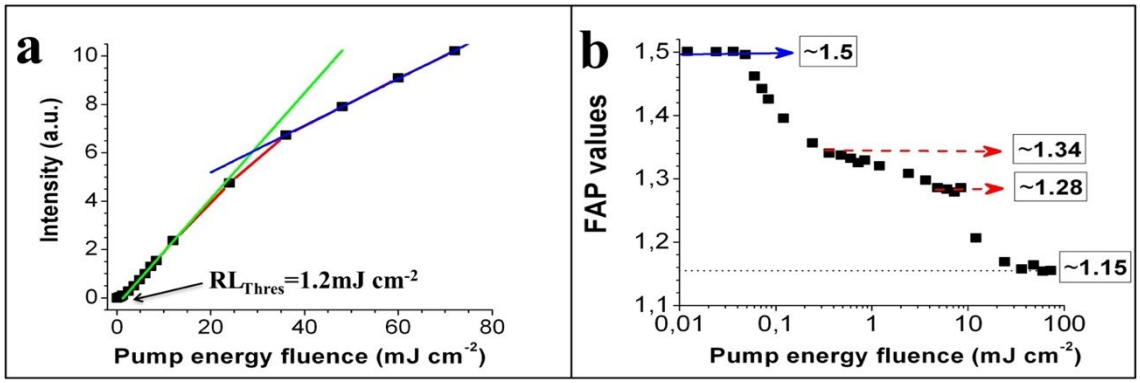

Figure 3. Influence of the pumping fluence on (a) the RL emitted peak intensity, RL_{eff}, for fluencies <12 mJ/cm^2 (green line) and >36 mJ/cm^2 (blue line) and (b) the *FAP* values, for fluencies <0.048 mJ/cm^2, FAP_{bT}≈1.5 (blue arrow).

Figure 3b shows *FAP* dependence with pumping energy fluence. The *FAP* value for fluencies <0.048 mJ/cm^2, well below the laser threshold (FAP_{bT}), was constant (~1.5). The *FAP* value decreases quickly for fluencies from 0.048 up to 0.36 mJ/cm^2. For fluencies between 0.36 and 4.8 mJ/cm^2, the *FAP* values decrease slowly from 1.34 down to 1.28, where it remains approximately constant up to a fluence of 8.4 mJ/cm^2. The *FAP* values start to drop quickly again for fluencies >8.4 mJ/cm^2 and decrease down to ~1.15 for fluencies ≥36 mJ/cm^2, showing a clear phase transition for the absorption, indicating two different modes of laser operation. From the FAP_{bT} value (1.5), we can estimate the average photon path length inside the scattering medium before being reflected (l_{eO}, equation 2), as well as the photon residence time (τ_{eO}, equation 3).

$$l_{eO} = \frac{l_a}{\left(\frac{1+\gamma_0}{2}\right)} \ln(FAP_{bT}) \approx \frac{384\ \mu m}{\left(\frac{1+1.84}{2}\right)} \times \ln(1.5) \approx 110\ \mu m \quad (2)$$

$$\tau_{eO} = \frac{l_{eO}}{c} n_{eff0} = \frac{l_{eO}}{c}\left(1 + \left(\frac{1+\gamma_0}{2}\right)(n_{eff} - 1)\right) \approx 110\ \mu m \times 3.3 \times 10^{-3}\ ps \times (1.75) \approx 0.64\ ps \quad (3)$$

where l_a, γ_0, n_{eff0}, n_{eff}, and c are the ballistic or microscopic absorption length [R6G], the enhanced absorption factor by localization (γ_0= 1.84) [44], the effective refractive index (increased by localization), the classical refractive index (1.53), and speed of light, respectively. The l_a value well below the laser threshold (passive regime) should not change (384 μm) at [10^{-4} M] of R6G. However, just as it was determined in our previous work [44], the absorption coefficient and the effective refractive index are enhanced near the input border $n_{eff0} = 1 + \left(\frac{1+\gamma_0}{2}\right)(n_{eff} - 1)$. The term $\left(\frac{1+\gamma_0}{2}\right) \approx \left(\frac{1+1.84}{2}\right) \approx 1.42$ represents an estimate of the mean value of the enhanced absorption factor in the region where absorption is enhanced. We note that l_{eo} is much lower than the microscopic absorption length of the scattering medium near the sample's surface (l_{ln0}) (residual absorption without R6G) determined in our previous work (l_{ln0} ≈2700 μm >>l_{eO}≈110 μm) [44]. Therefore, the photons would leave the scattering medium long before being absorbed by it. The observed saturated absorption (fig. 1b) can be explained in the following way: a very low percentage of R6G molecules are in the lowest sublevels, S_{0i}, of the ground state, and/or a high population of molecules are in the sublevels, S_{1i}, of the excited singlet state. Saturated emission (fig. 1a) means a low population of molecules are in the lowest sublevels, S_{1i}, of the excited singlet state or/and a high population are in the S_{0i} sublevels of the ground state. Joining saturated absorption and saturated emission, the result is that a large percentage of R6G molecules are encountered in the higher lying sublevels of S_1 and S_0. Therefore, the transition rates from S_{0i} up to S_{1i} (absorption) and from S_{1i} to S_{0i} (stimulated emission) are higher than the vibrational relaxation rate within the excited singlet sublevels, S_{1i}, or within the sublevels of the ground state, S_{0i}. The polarization of R6G molecules by pumping photons trapped within localized states should give rise to a photon-molecule bound state [7,48], which in turn would lead to the suppression of vibrational relaxation [49] and spontaneous emission [50].

3.3.2 Random laser action in a small micrometric volume

When collecting the light from the front side of the sample coming from a large surface area as before in Chapter 3.3.1, the emission of localized modes is integrated, making its individual detection difficult. Therefore, to better analyze the possible peaks, a study has been performed collecting RL emissions from a micrometric region (~3.8 μm diameter) near the input-pumping surface (less than 4 μm depth) using a detection system that performs like a confocal microscope [51]. Figure 4a, b, c and d show the evolution of the emission spectra for pumping fluencies below 0.8 mJ/cm^2 , close to 1.2 mJ/cm^2, and above the RL threshold, 3.2 and 7.2 mJ/cm^2, respectively. The spectral region framed with a dashed circle highlights the emerging peaks. For lower pumping fluencies (0.8 mJ/cm^2), the spectra consisted of the fluorescence emission band with overlapping narrow peaks at frequencies close to the maximum of the spectrum. As the pump fluence increases, the emission band becomes narrower, although the overlapped narrow peaks continue to appear in approximately the same frequency interval of 15−20 nm. The minimum linewidth observed for the narrowest peaks was ≤0.17 nm, which is the spectral resolution limit of our detection system. However, the photon residence time, determined by *FAP* measurement (τ_{eO}≈ 0.64 ps; equation 3), would yield a homogeneous spectral broadening of ~1.29 nm, obtained by using a Fourier transform assuming a Gaussian envelope, which is broader than this narrowest linewidth (≤0.17 nm). This fact could be a consequence of an anomalous nonlinear increase of the refractive index within the closed loop paths (localized states), which gives rise to a phase shift (for the pumping photon) that continuously increases by increasing the intensity (within the closed loop paths), during the residence time of the pumping photons. This phase accumulated by *pumping photons* can lead to a resonance breaking, reducing τ_{eO}. However, for *emitted photons* this phase accumulation by such an anomalous nonlinear effect would be greatly suppressed above the lasing threshold, as the intensity increase for each lasing mode would be a consequence of the stimulated emission. In other words, the phase accumulated within the localized state during the laser action (emission) by nonlinear effects is corrected continually, as the intensity increase results from the stimulated emission. Perhaps for this reason, the coherent laser emission sustained by localization has been largely recognized in disordered optical media with gain [31,34,52,53]. However, the direct observation of localization in the absence of gain has proved to be elusive [54,55]. In this way, an anomalous nonlinear increase of the refractive index could be a likely cause, by which pump photons leave the scattering medium, breaking the interference condition (localization). This can be interpreted as photon-photon (virtual) interaction, due to the strong photon correlation within a localized state [49], which in turn can also be understood as that the average of the electromagnetic

field at any point within a localized state ceases to be zero. A similar nonlinear phenomenon was theoretically addressed by Buttiker and Moskalets in disordered electronic media [56], who proposed that when the energy of the localized state changes, the localized state can emit nonequilibrium electrons and holes propagating away from the localized state within the edge state, which acts similar to a waveguide. The position of these sharp peaks changes little in a few seconds; it only changes completely after tens of seconds or by stirring the sample. Notice that the pump spot is 3 mm in diameter, and the estimated pump depth above the RL threshold must be around 15 μm. Therefore, the effects caused by inhomogeneous pumping should not play a role in promoting these peaks. In addition, the narrow peaks could not result from amplified spontaneous emission [37], as these emission spectra are obtained by integrating 21 laser shots of long duration (~4 ns).

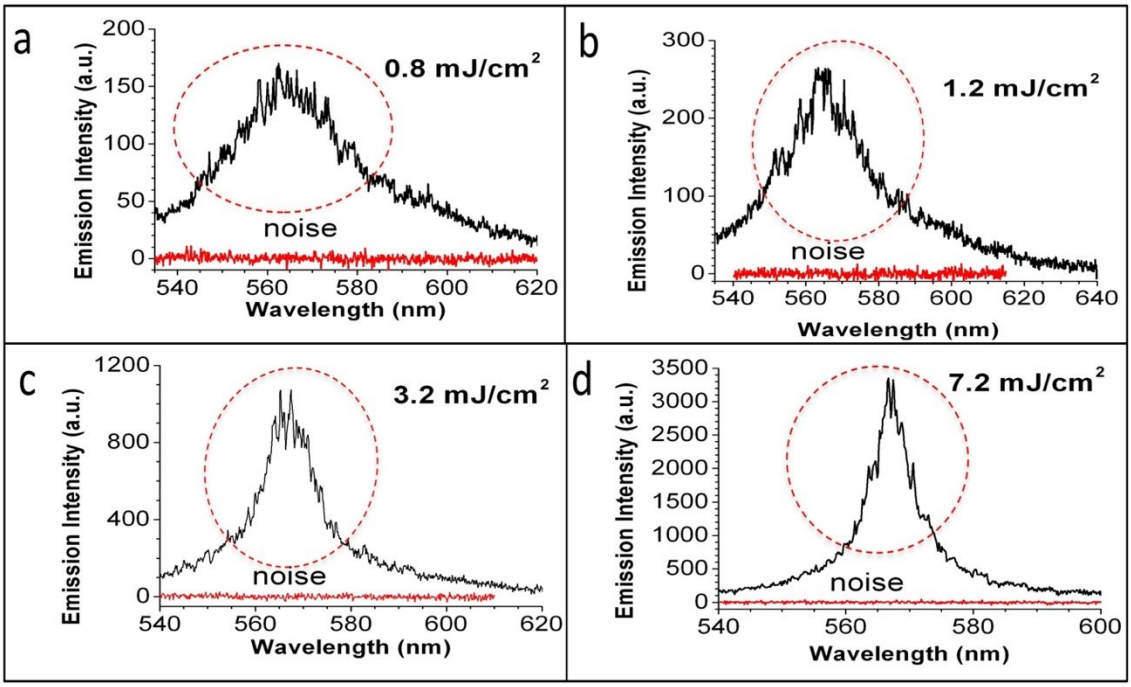

Figure 4. Emission spectra of RL collected from a small micrometric volume (<4 μm diameter and depth) for pumping fluencies of (a) 0.8, (b) 1.2, (c) 3.2, and (d) 7.2 mJ/cm^2. The diameter of the pumping spot is the same (3 mm). The solid red lines represent the respective noise signal. The dashed red circles highlight peaks emerging in the RL emission spectrum. Emission spectra were collected integrating 21 laser shots.

We note that the intensity of these narrow peaks, relative to the fluorescence band, is lower than that reported by Cao and co-workers [31] that could be a consequence of the extremely reduced (effective) size of their random laser composed of ZnO nanoparticles of 50 nm clustered in micrometric structures (diameter of several micrometers): it is known that the density of strongly localized modes (anomalous or superficial localized modes, long lifetime) increases in the vicinity of the boundary, which was theoretically predicted by Mirlin in disordered electronic media [57,58]. The anomalous or superficial localized modes are those where the boundary is part of the closed loop path (localized state). Thereby, the density of superficial localized modes (long lifetime) must increase and the total amount of localized modes decrease as system size is decreased below localization length. The latter can be interpreted as an increase in the extent of localization (modes of long lifetime, decrease of the effective localization length) for a reduced number of anomalous localized modes (decrease of the total amount of localized modes) within these micrometric clusters. Additionally, an increase of the effective refractive index is expected near the boundaries (localization) [44,59]. Consequently, owing to the fact that surface-volume ratio is considerably higher in these clusters; the interference (localization) must be increased, since the photon pathlength is forced to be longer due to the internal reflection. The latter can be understood such that the presence of a finite barrier in the border provokes an increase of the quantum interference (localization), which was theoretically demonstrated by Ramos and co-workers in disordered electronic media [60]. Therefore, lasing emission in their sample (clusters) must be confined to fewer lasing modes (anomalous localized modes) with higher intensity (high quality factor, long lifetime) [61]. However, our sample is a three-dimensional (3D) semi-infinite system with just one effective border, the input interface (silica-sample). On the other hand, contrary to our sample, where an R6G quantum

efficiency near unity is expected, the fluorescence in their sample must be greatly quenched due to the superficial defects and dangling bonds of ZnO nanoparticles. Nevertheless, the excitation of ZnO or R6G molecules within the closed loop paths (excitation within localized state) would be free of quenching, since such molecules would be strongly correlated [49]. Therefore, the intensity ratio (peaks/ fluorescence) reported by Cao and co-workers (clusters) [31] must be necessarily greater than that observed in our sample. In this way, the system studied by Cao and co-workers (very small size) [31] should be addressed as a particular case of random lasing at localization or localization transition for reduced size. Indeed, in a subsequent study conducted by the same group [52], ZnO spheres of 85-617 nm diameters were cold pressed to form pellets. In this case, the relative intensity of the sharp peaks was considerably lower and for the sample of 85 nm spheres, lasing was not observed, which was attributed to a drastic increase of the random laser's cavity size brought about by an increase in transport mean free path. The latter indicates that the clustered structure (composed by 50 nm Nps) with very small dimensions (micrometric) [31] must play a crucial role in the localized lasing phenomenon. The above perspective represents another approach to addressing the random lasing at localization, since the shape and size of a random laser should have strong influence on localization and consequently on random lasing.

3.3.3 Study of Random laser modes

To determine the contribution of the RL modes, the superfluorescence band (extended band mode or ASE) and the narrow peaks (peaks mode), an additional experiment was designed. Let us introduce the following conjecture: if the narrow peaks are derived from localized modes due to the localization phenomenon, then they should basically be backscattered, that is, their emission should be detected in the direction opposite to the pump direction. Note that the emission of localized modes inside the sample is exponentially attenuated, so that if they are very near the front edge, they will be detected only in the spectrum obtained from the front surface (frontal spectrum) because they are too far from the back edge to survive, as the attenuation is huge. During the experiment, the RL emission was also collected from the back of the cuvette (back collection). The back-collected spectra consisted of a broad emission band (~50 nm bandwidth) with an overlapped single emission band, whose intensity and bandwidth are dependent on the pumping energy [51].

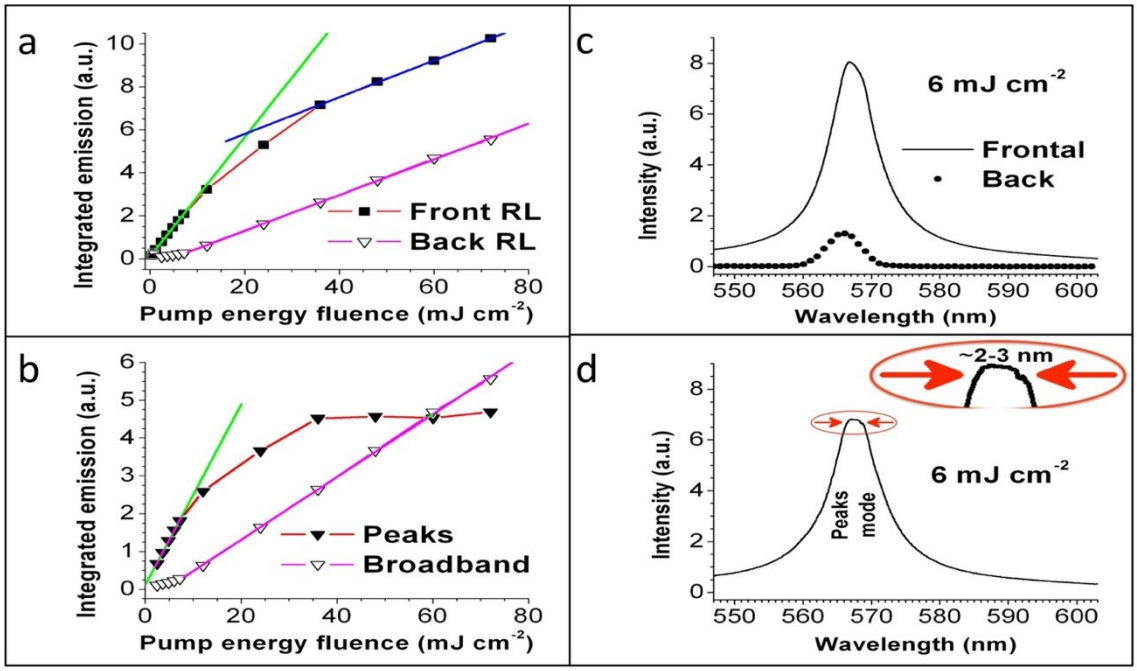

Figure 5. Influence of the pump fluence on (a) the spectrally integrated emission intensity for frontal and back collection, (b) spectrally integrated emission intensity of RL back collection (open triangle) and difference between frontal and back collection (closed triangle). (c) The emission spectra for a fluence of 6 mJ/cm^2 collected at the back (dots) and front (line) of the cuvette, and (d) difference between the frontal and back spectra of (c).

Figure 5a shows the behavior of the spectrally integrated RL emission for the frontal integrated collection (collected over the whole emission volume) and back collection. Figure 5b shows a comparison of the spectrally integrated RL

emissions for peaks and band modes. The integrated emission slope (fluencies ≤ 8.4 mJ/cm^2) of the peaks mode (green line) was ~2.9 times higher than that for the extended mode band (magenta line). Therefore, for fluencies ≤8.4 mJ/cm^2, ~74% of the RL emission, detected with our experimental setup, corresponds to the peaks mode. Figure 5c shows the RL emission spectra at 6 mJ/cm^2 for both collections, the frontal spectrum collected over the whole emission volume and the back spectrum. The bandwidth of the frontal spectrum (8.8 nm) is larger than that of the back spectrum (4.8 nm). In addition, the frontal spectra are slightly asymmetrical, showing a widening toward a longer wavelength. The resulting spectrum from the difference between both spectra (Figure 5d), which must correspond to the emission spectrum of the peaks mode collected from the whole emission area (integrated collection), shows a plateau in intensity of 2-3 nm. This indicates suppression of the interaction between the peaks modes, which is a signature of random lasing at localization [34,43].

4. CONCLUSION

The core-shell TiO_2@Silica nanoparticle for a random laser combines the high refractive index of TiO_2 with chemical inertness, "optical" colloidal stability (steric "optical" effect), and better light coupling (TiO_2 cores) provided by the silica shell. Higher efficiency, lower RL threshold and lower photodegradation in the random laser were achieved. The *FAP* measurement could be a promising method to characterize scattering media. The core-shell TiO_2@Silica nanoparticle at [140x10^{10} NPs ml^{-1}], allowed us to study the RL action at the critical regime of approaching localization. An absorption-emission saturation phenomenon was observed in the RL. This phenomenon was associated with the absorption-emission saturation of the localized modes called the peaks mode. Narrow peaks with a linewidth of ≤0.17 nm were observed in the RL emission spectrum. This linewidth (≤0.17 nm) is narrower than the mean linewidth of the modes of the scattering medium (~1.29 nm, $\tau_{e0} \approx$ 0.64 ps). This fact could be a consequence of the anomalous nonlinear increase of the refractive index by localization, due to the continuously increasing intensity within the closed loop paths during the residence time of the pumping photons. This effect would be greatly suppressed for emitted photons above the lasing threshold, as the intensity increase would be a result of stimulated emission. The back-collection method allowed for the separate measurement of the RL band mode, showing a linear dependence with pumping fluence without gain depletion. The core-shell strategy presented and discussed in this paper could enable the design, manufacture and characterization of novel optical devices, based on highly disordered scattering media.

ACKNOWLEDGEMENTS

We acknowledge financial support from FACEPE, CNPq and FAPESP (grants 2017 05854-9 and 2017 10765-5).

REFERENCES

[1] Genovese, M. P., Lightcap, I. V. and Kamat, P. V., "Sun-Believable Solar Paint. A Transformative One-Step Approach for Designing Nanocrystalline Solar Cells," ACS Nano **6**(1), 865–872 (2012).

[2] Wetter, N. U., Giehl, J. M., Butzbach, F., Anacleto, D. and Jiménez-Villar, E., "Polydispersed Powders (Nd 3+ :YVO 4) for Ultra Efficient Random Lasers," Part. Part. Syst. Charact., 1700335 (2017).

[3] Vieira, R. J. R., Gomes, L., Martinelli, J. R. and Wetter, N. U., "Upconversion luminescence and decay kinetics in a diode-pumped nanocrystalline Nd^3+:YVO_4 random laser," Opt. Express **20**(11), 12487 (2012).

[4] Jorge, K. C., Alvarado, M. A., Melo, E. G., Carreño, M. N. P., Alayo, M. I. and Wetter, N. U., "Directional random laser source consisting of a HC-ARROW reservoir connected to channels for spectroscopic analysis in microfluidic devices," Appl. Opt. **55**(20), 5393 (2016).

[5] John, S., "Electromagnetic absorption in a disordered medium near a photon mobility edge," Phys. Rev. Lett. **53**(22), 2169–2172 (1984).

[6] John, S., "Strong localization of photons in certain disordered dielectric superlattices," Phys. Rev. Lett. **58**(23), 2486–2489 (1987).

[7] John, S., "Localization of Light," Phys. Today **44**(5), 32 (1991).

[8] John, S., "Why trap light?," Nat. Mater. **11**(12), 997–999 (2012).

[9] SoljaČiĆ, M. and Joannopoulos, J. D., "Enhancement of nonlinear effects using photonic crystals," Nat. Mater. **3**(4), 211–219 (2004).

[10] Abderrafi, K., Jiménez, E., Ben, T., Molina, S. I., Ibáñez, R., Chirvony, V. and Martínez-Pastor, J. P., "Production of Nanometer-Size GaAs Nanocristals by Nanosecond Laser Ablation in Liquid," J. Nanosci. Nanotechnol. **12**(8), 6774–6778 (2012).

[11] Jimenez-Villar, E., Mestre, V., de Oliveira, P. C. and de Sá, G. F., "Novel core–shell (TiO2@Silica)

nanoparticles for scattering medium in a random laser: higher efficiency, lower laser threshold and lower photodegradation," Nanoscale **5**(24), 12512 (2013).
[12] Jimenez-Villar, E., Mestre, V., de Oliveira, P. C., Faustino, W. M., Silva, D. S. and de Sá, G. F., "TiO 2 @Silica nanoparticles in a random laser: Strong relationship of silica shell thickness on scattering medium properties and random laser performance," Appl. Phys. Lett. **104**(8), 81909 (2014).
[13] Rodriguez, E., Jimenez, E., Jacob, G. J., Neves, A. A. R., Cesar, C. L. and Barbosa, L. C., "Fabrication and characterization of a PbTe quantum dots multilayer structure," Phys. E Low-dimensional Syst. Nanostructures **26**(1–4), 361–365 (2005).
[14] Rodriguez, E., Kellermann, G., Craievich, A. F., Jimenez, E., César, C. L. and Barbosa, L. C., "All-optical switching device for infrared based on PbTe quantum dots," Superlattices Microstruct. **43**(5–6), 626–634 (2008).
[15] Jiménez, E., Abderrafi, K., Abargues, R., Valdés, J. L. and Martínez-Pastor, J. P., "Laser-Ablation-Induced Synthesis of SiO 2 -Capped Noble Metal Nanoparticles in a Single Step," Langmuir **26**(10), 7458–7463 (2010).
[16] Jiménez, E., Abderrafi, K., Martínez-Pastor, J., Abargues, R., Luís Valdés, J. and Ibáñez, R., "A novel method of nanocrystal fabrication based on laser ablation in liquid environment," Superlattices Microstruct. **43**(5–6), 487–493 (2008).
[17] González-Castillo, J. R., Rodriguez, E., Jimenez-Villar, E., Rodríguez, D., Salomon-García, I., de Sá, G. F., García-Fernández, T., Almeida, D. B., Cesar, C. L., Johnes, R. and Ibarra, J. C., "Synthesis of Ag@Silica Nanoparticles by Assisted Laser Ablation," Nanoscale Res. Lett. **10**(1), 399 (2015).
[18] González-Castillo, J. R., Rodríguez-González, E., Jiménez-Villar, E., Cesar, C. L. and Andrade-Arvizu, J. A., "Assisted laser ablation: silver/gold nanostructures coated with silica," Appl. Nanosci. **7**(8), 597–605 (2017).
[19] Ermakov, V. A., Jimenez-Villar, E., Silva Filho, J. M. C. da, Yassitepe, E., Mogili, N. V. V., Iikawa, F., de Sá, G. F., Cesar, C. L. and Marques, F. C., "Size Control of Silver-Core/Silica-Shell Nanoparticles Fabricated by Laser-Ablation-Assisted Chemical Reduction," Langmuir **33**(9), 2257–2262 (2017).
[20] Sánchez-Muñoz, O. L., Salgado, J., Martínez-Pastor, J. and Jiménez-Villar, E., "Synthesis and Physical Stability of Novel Au-Ag@SiO2 Alloy Nanoparticles," Nanosci. Nanotechnol. **2**(1), 1–7 (2012).
[21] Fuertes, G., Sánchez-Muñoz, O. L., Pedrueza, E., Abderrafi, K., Salgado, J. and Jiménez, E., "Switchable Bactericidal Effects from Novel Silica-Coated Silver Nanoparticles Mediated by Light Irradiation," Langmuir **27**(6), 2826–2833 (2011).
[22] Fuertes, G., Pedrueza, E., Abderrafi, K., Abargues, R., Sánchez, O., Martínez-Pastor, J., Salgado, J. and Jiménez, E., "Photoswitchable bactericidal effects from novel silica-coated silver nanoparticles," Prog. Biomed. Opt. Imaging - Proc. SPIE **8092**, R. Sroka and L. D. Lilge, Eds., 80921M (2011).
[23] Rodríguez, E., Jimenez, E., Padilha, L. A., Neves, A. A. R., Jacob, G. J., César, C. L. and Barbosa, L. C., "SiO2/PbTe quantum-dot multilayer production and characterization," Appl. Phys. Lett. **86**(11), 113117 (2005).
[24] Kellermann, G., Rodriguez, E., Jimenez, E., Cesar, C. L., Barbosa, L. C. and Craievich, A. F., "Structure of PbTe(SiO 2)/SiO 2 multilayers deposited on Si(111)," J. Appl. Crystallogr. **43**(3), 385–393 (2010).
[25] Rodríguez, E., Jimenez, E., Cesar, C. L., Barbosa, L. C. and De Araújo, C. B., "1D photonic band gap PbTe doped silica quantum dot optical device," Glas. Technol. **46**(2), 47–49(3) (2005).
[26] Letokhov, V. S., "Generation of Light by a Scattering Medium with Negative Resonance Absorption," J. Exp. Theor. Phys. **26**(4), 835 (1968).
[27] Noginov, M. A., [Solid-State Random Lasers], Springer-Verlag, New York (2005).
[28] Cao, H., "Review on latest developments in random lasers with coherent feedback," J. Phys. A. Math. Gen. **38**(49), 10497–10535 (2005).
[29] Wiersma, D. S., "The physics and applications of random lasers," Nat. Phys. **4**(5), 359–367 (2008).
[30] Lawandy, N. M., Balachandran, R. M., Gomes, A. S. L. and Sauvain, E., "Laser action in strongly scattering media," Nature **368**(6470), 436–438 (1994).
[31] Cao, H., Zhao, Y. G., Ho, S. T., Seelig, E. W., Wang, Q. H. and Chang, R. P. H., "Random Laser Action in Semiconductor Powder," Phys. Rev. Lett. **82**(11), 2278–2281 (1999).
[32] van der Molen, K. L., Tjerkstra, R. W., Mosk, A. P. and Lagendijk, A., "Spatial Extent of Random Laser Modes," Phys. Rev. Lett. **98**(14), 143901 (2007).
[33] Leonetti, M. and Lopez, C., "Random lasing in structures with multi-scale transport properties," Appl. Phys. Lett. **101**(25), 251120 (2012).
[34] Liu, J., Garcia, P. D., Ek, S., Gregersen, N., Suhr, T., Schubert, M., Mørk, J., Stobbe, S. and Lodahl, P., "Random nanolasing in the Anderson localized regime," Nat. Nanotechnol. **9**(4), 285–289 (2014).
[35] Conti, C. and Fratalocchi, A., "Dynamic light diffusion, three-dimensional Anderson localization and lasing in

inverted opals," Nat. Phys. **4**(10), 794–798 (2008).
[36] Polson, R. C., Chipouline, A. and Vardeny, Z. V., "Random Lasing in π-Conjugated Films and Infiltrated Opals," Adv. Mater. **13**(10), 760–764 (2001).
[37] Mujumdar, S., Ricci, M., Torre, R. and Wiersma, D. S., "Amplified extended modes in random lasers," Phys. Rev. Lett. **93**(5), 1–4 (2004).
[38] Wu, X., Andreasen, J., Cao, H. and Yamilov, A., "Effect of local pumping on random laser modes in one dimension," J. Opt. Soc. Am. B **24**(10), A26 (2007).
[39] Wu, X. and Cao, H., "Statistical studies of random-lasing modes and amplified spontaneous-emission spikes in weakly scattering systems," Phys. Rev. A - At. Mol. Opt. Phys. **77**(1), 1–10 (2008).
[40] Tureci, H. E., Ge, L., Rotter, S. and Stone, A. D., "Strong Interactions in Multimode Random Lasers," Science (80-.). **320**(5876), 643–646 (2008).
[41] Zaitsev, O. and Deych, L., "Recent developments in the theory of multimode random lasers," J. Opt. **12**(2), 24001 (2010).
[42] Cao, H., Xu, J. Y., Zhang, D. Z., Chang, S. H., Ho, S. T., Seelig, E. W., Liu, X. and Chang, R. P. H., "Spatial confinement of laser light in active random media," Phys. Rev. Lett. **84**(24), 5584–5587 (2000).
[43] Stano, P. and Jacquod, P., "Suppression of interactions in multimode random lasers in the Anderson localized regime," Nat. Photonics **7**(1), 66–71 (2013).
[44] Jimenez-Villar, E., da Silva, I. F., Mestre, V., de Oliveira, P. C., Faustino, W. M. and de Sá, G. F., "Anderson localization of light in a colloidal suspension (TiO 2 @silica)," Nanoscale **8**(21), 10938–10946 (2016).
[45] Wold, A., "Photocatalytic properties of titanium dioxide (TiO2)," Chem. Mater. **5**(3), 280–283 (1993).
[46] Tsukamoto, M., Abe, N., Soga, Y., Yoshida, M., Nakano, H., Fujita, M. and Akedo, J., "Control of electrical resistance of TiO2 films by short-pulse laser irradiation," Appl. Phys. A **93**(1), 193–196 (2008).
[47] Gerischer, H. and Heller, A., "The role of oxygen in photooxidation of organic molecules on semiconductor particles," J. Phys. Chem. **95**(13), 5261–5267 (1991).
[48] John, S. and Wang, J., "Quantum electrodynamics near a photonic band gap: Photon bound states and dressed atoms," Phys. Rev. Lett. **64**(20), 2418–2421 (1990).
[49] John, S. and Wang, J., "Quantum optics of localized light in a photonic band gap," Phys. Rev. B **43**(16), 12772–12789 (1991).
[50] Yablonovitch, E., "Inhibited spontaneous emission in solid-state physics and electronics," Phys. Rev. Lett. **58**(20), 2059–2062 (1987).
[51] Jiménez-Villar, E., da Silva, I. F., Mestre, V., Wetter, N. U., Lopez, C., de Oliveira, P. C., Faustino, W. M. and de Sá, G. F., "Random Lasing at Localization Transition in a Colloidal Suspension (TiO 2 @Silica)," ACS Omega **2**(6), 2415–2421 (2017).
[52] Wu, X. H., Yamilov, A., Noh, H., Cao, H., Seelig, E. W. and Chang, R. P. H., "Random lasing in closely packed resonant scatterers," J. Opt. Soc. Am. B **21**(1), 159–167 (2004).
[53] Noginov, M. A., Zhu, G., Belgrave, A. M., Bakker, R., Shalaev, V. M., Narimanov, E. E., Stout, S., Herz, E., Suteewong, T. and Wiesner, U., "Demonstration of a spaser-based nanolaser," Nature **460**(7259), 1110–1112 (2009).
[54] Wiersma, D. S., Bartolini, P., Lagendijk, A. and Righini, R., "Localization of light in a disordered medium," Nature **390**(6661), 671–673 (1997).
[55] Sperling, T., Bührer, W., Aegerter, C. M. and Maret, G., "Direct determination of the transition to localization of light in three dimensions," Nat. Photonics **7**(1), 48–52 (2013).
[56] Büttiker, M. and Moskalets, M., "FROM ANDERSON LOCALIZATION TO MESOSCOPIC PHYSICS," Int. J. Mod. Phys. B **24**(12n13), 1555–1576 (2010).
[57] Mirlin, A. D., "Spatial structure of anomalously localized states in disordered conductors," J. Math. Phys. **38**(4), 1888–1917 (1997).
[58] Mirlin, A., "Statistics of energy levels and eigenfunctions in disordered systems," Phys. Rep. **326**(5–6), 259–382 (2000).
[59] Campagnano, G. and Nazarov, Y. V., "G(Q) corrections in the circuit theory of quantum transport," Phys. Rev. B **74**(12), 1–15 (2006).
[60] Barbosa, A. L. R., Bazeia, D. and Ramos, J. G. G. S., "Universal Braess paradox in open quantum dots," Phys. Rev. E **90**(4), 42915 (2014).
[61] Jimenez-Villar, E., Xavier, M. C. S., Mestre, V., Martins, W. S., Basso, G. F., Wetter, N. U. and de Sa, G. F., "Anderson localization of light: Strong dependence with incident angle" (2017).